BEARING STRENGTH PREDICTION BY CFRP AND FFRP DAMAGE ONSET CRITERIA FOR RIVETED JOINTS

Jarno Jokinen[a], Oscar Rodera Garcia[a], Pauli Hakala[a], Farzin Javanshour[a], Mikko Kanerva[a]*

a: Faculty of Engineering and Natural Sciences, Tampere University, Finland
* Corresponding author: jarno.jokinen@tuni.fi

Abstract: *Fasteners are a typical method for providing load transfer between different parts. The current interest by the industry is to use natural fibres, such as flax, in composite laminates. The failure modes in flax fibre reinforced plastic (FRP) composite joints are clearly less known. This work studies the damage onset of a fastener joint using three-dimensional finite element models. The damage onset is analysed using the Hashin 3D and Puck's failure criterion. In the analysis, carbon and flax FRP joints are simulated. The analyses remark that the Puck criterion's parameters have an influence on the damage onset and specific parameters are needed for the flax FRP in joints.*

Keywords: bearing; joint; Hashin; Puck; flax

1. Introduction

Mechanical joints are a critical part in lightweight composite structures. Mechanical joints have several advantages, which include applicability to inspections and disassembly. The challenge is the stress peaks caused by fasteners. For studying the load-carrying capability of these mechanical joints, both analytical and numerical methods are used. These are mainly based on stress-based methodologies. The stress field around the fastener in orthotropic composite plies is complex and requires a fitting failure criterion for taking into account different stress components. Several different stress and strain-based criteria have been developed [1].

In addition to strength values, certain criterion includes parameters dependent on the laminate. This is a challenge when new material combinations are taken into use. The current trend of many industrial fields is sustainability, which evokes further interest in natural engineering materials, such as flax fibres. Currently, there is no long-term experience about the using of flax laminates in the structural applications, including mechanical joints [2,3].

The target of this work is to study the damage onset in carbon fibre reinforced plastic (CFRP) and flax fibre reinforced plastic (FFRP) laminate joints with fasteners. The study is performed using finite element (FE) analyses where Hashin 3D and Puck criteria are implemented. The work compares the damage onset and studies the influence of Puck criterion's parameters. In addition, the location of the damage and the influence of friction are covered.

2. Methods

2.1 Finite element model

The three-dimensional FE model presenting a riveted joint was created using Abaqus/Standard 2021 (Fig. 1). The model consisted of three laminates and one rivet. All three laminates had the same geometry (length 48 mm and width 24 mm). The rivet diameter was 4 mm. The simplicity

  doi:10.5075/epfl-298799_978-2-9701614-0-0

of the fastener was considered, e.g. countersinks were not modelled. The circular fastener ends (heads) had 8 mm outside the hole region (1 mm in thickness). The 'rivet edge' distance was 12 mm in the longitudinal direction and 12 mm in the width direction. Eight ply laminates' stacking sequence was $[0/45/-45/90]_{SE}$. The thicknesses of CFRP and FFRP laminates were respectively 1.12 mm and 2.96 mm. The 0-direction was parallel to the loading direction. The ply properties for CFRP and FFRP are presented in Table 1.

Table 1: Material properties used in this study. [4–6]

	CFRP	FFRP
Ply thickness [mm]	0.14	0.37
E_1 [GPa]	140	24.98
E_2, E_3 [GPa]	10	4.51
ν_{12}, ν_{13}, ν_{23}	0.3	0.3
G_{12}, G_{13}, G_{23} [GPa]	5.17	5.21
X_T [MPa]	2080	260
X_C [MPa]	1560	260
Y_T, Z_T [MPa]	59	18.58
Y_C, Z_C [MPa]	203	18.58
S (S_{12},S_{13},S_{23}) [MPa]	93	33.51
E_f [GPa]	230	58.9
E_m [GPa]	3	2.9

The laminates were connected using a titanium fastener. The fastener's Young's modulus was 110 GPa, and Poisson's ratio was 0.3. The contacts between fastener and laminates and laminate and laminate were modelled. These contacts were modelled as frictionless and frictional. The effects of fastener tightening were also covered in the numerical analyses. The tightening effect was modelled by pressure loading at the fastener socket region.

The FE models were loaded by tensile loading simulating the mechanical load. The loading was performed using the enforced displacement at the left side edge of the middle laminate. The (same) edge width and vertical displacements were restricted. The value of enforced displacement was 0.1 mm in the CFRP joint and 0.05 mm in the FFRP joint. The outside laminates were restricted in all the three directions at the laminate end edge, as shown in Figure 1. The FE model laminates were modelled using fully integrated solid elements (C3D8) and the rivet using reduced integrated solid elements (C3D8R). The typical element dimension was 1 mm, which provided approximately 28,000 elements for the CFRP and FFRP models.

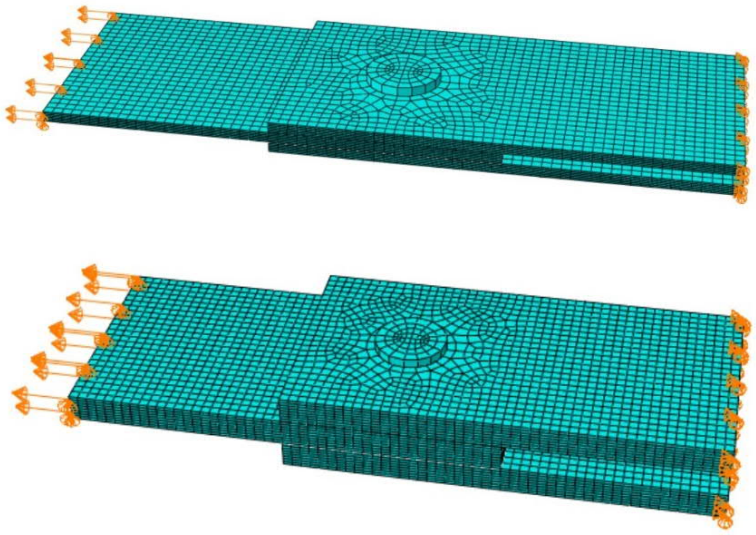

Figure 1. The finite element models of the CFRP (top) and the FFRP (bottom) joints.

2.2 Damage onset criterion

The damage onset for the joint laminates was studied using the Hashin 3D and Puck stress criteria [7,8]. Both criteria were implemented to the analysis using the user-defined material subroutine (UMAT) in Abaqus [9]. The Hashin 3D and Puck criteria can be extracted in the following form:

Hashin 3D Fibre failure

$$f_{FF} = \left(\frac{\sigma_{11}}{X_T}\right)^2 + \left(\frac{\sigma_{12}}{S}\right)^2 + \left(\frac{\sigma_{13}}{S}\right)^2, \text{when } \sigma_{11} > 0 \quad (1)$$

$$f_{FF} = \left(\frac{\sigma_{11}}{X_C}\right)^2, \text{when } \sigma_{11} < 0 \quad (2)$$

Hashin 3D Matrix Failure

$$f_{IFF} = \left(\frac{\sigma_{22}+\sigma_{33}}{Y_T}\right)^2 + \frac{\sigma_{23}^2-\sigma_{22}\cdot\sigma_{33}}{S^2} + \frac{\sigma_{12}^2+\sigma_{13}^2}{S^2}, \text{when } \sigma_{22} + \sigma_{33} > 0 \quad (3)$$

$$f_{IFF} = \frac{1}{Y_C}\left[\left(\frac{Y_C}{2S}\right)^2 - 1\right](\sigma_{22} + \sigma_{33}) + \frac{(\sigma_{22}+\sigma_{33})^2}{4S^2} + \frac{(\sigma_{23}^2-\sigma_{22}\sigma_{33})}{S^2} + \frac{(\sigma_{12}^2+\sigma_{13}^2)}{S^2}, \text{ when } (\sigma_{22} + \sigma_{33} < 0) \quad (4)$$

Puck Fibre failure

$$f_{EFF} = \frac{1}{R_{\parallel}^{t,c}}\left[\sigma_{11} - \left(\nu_{\perp\parallel} - \nu_{\perp\parallel f} m_{\sigma_1}\frac{E_{\parallel}}{E_{\parallel f}}\right)(\sigma_{22} + \sigma_{33})\right] = 1, \text{when } \sigma_{11} > 0 \quad (5)$$

$$f_{EFF} = \frac{1}{-R_{\parallel}^{t,c}}\left[\sigma_{11} - \left(\nu_{\perp\parallel} - \nu_{\perp\parallel f} m_{\sigma_1}\frac{E_{\parallel}}{E_{\parallel f}}\right)(\sigma_{22} + \sigma_{33})\right] = 1, \text{when } \sigma_{11} < 0 \quad (6)$$

Puck Matrix failure

$$f_{EIFF} = \sqrt{\left(\left(\frac{1}{R_{\perp}^{At}} - \frac{p_{\perp\psi}^t}{R_{\perp\psi}^A}\right)\sigma_n(\theta)\right)^2 + \left(\frac{\tau_{nt}(\theta)}{R_{\perp\perp}^A}\right)^2 + \left(\frac{\tau_{n1}(\theta)}{R_{\perp\parallel}^A}\right)^2} + \frac{p_{\perp\psi}^t}{R_{\perp\psi}^A}\sigma_n(\theta), \text{when } \sigma_n(\theta) > 0 \quad (7)$$

$$f_{EIFF} = \sqrt{\left(\left(\frac{1}{R_{\perp}^{At}} - \frac{p_{\perp\psi}^{t}}{R_{\perp\psi}^{A}}\right)\sigma_n(\theta)\right)^2 + \left(\frac{\tau_{nt}(\theta)}{R_{\perp\perp}^{A}}\right)^2 + \left(\frac{\tau_{n1}(\theta)}{R_{\perp\parallel}^{A}}\right)^2} + \frac{p_{\perp\psi}^{t}}{R_{\perp\psi}^{A}}\sigma_n(\theta), \text{when } \sigma_n(\theta) > 0 \quad (8)$$

$$\text{with } \frac{p_{\perp\psi}^{t,c}}{R_{\perp\psi}^{A}} = \frac{p_{\perp\perp}^{t,c}}{R_{\perp\perp}^{A}}\cos^2\psi + \frac{p_{\perp\parallel}^{t,c}}{R_{\perp\parallel}^{A}}\sin^2\psi. \quad (9)$$

Puck criterion's $p_{\perp\parallel}^{t}$, $p_{\perp\parallel}^{c}$, $p_{\perp\parallel}^{t}$ and $p_{\perp\parallel}^{c}$ were modified during the analyses. For the detailed description of the Puck and Hashin parameters, the work by Rodera Garcia [9] is referred.

3. Results

3.1 Stress distributions

The analyses were performed using the enforced displacement, and the corresponding reaction forces were calculated at laminate ends (Table 2). The bearing and by-pass stresses were evaluated in the middle laminate, which had a higher loading than the outside (strap) laminates. The bearing stress can be estimated based on the simplified analytical equation

$$\sigma_{BR} = P/dt \quad (10)$$

where P is the force, d is the fastener diameter, and t is the adherend thickness. The by-pass stresses were estimated using the area based on the laminate width excluding rivet hole and multiplied by laminate thickness.

Table 2: Joint reaction forces, average bearing, and by-pass stress in this study.

	CFRP	FFRP
Reaction force [N]	1124	400
Bearing stress [MPa]	251	34
By-pass stress [MPa]	50	7

3.2 Hashin failure criterion

Firstly, the damage onset was studied using the Hashin failure criterion. The values were evaluated in three nodal lines (A, B and C) in the middle laminate, as shown in Figure 2. The nodal (lines) locations had an angle (of 0, 54 and 90) over the loading direction. The failure criterion's values were studied in these locations for different ply orientations.

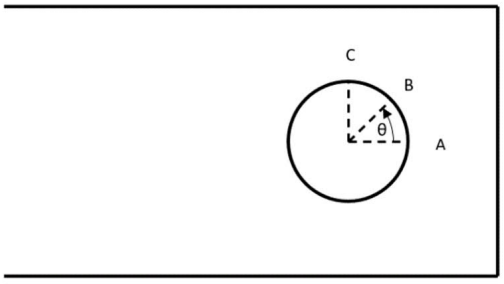

Figure 2. Nodal lines in the middle laminate.

The margin of safety (MoS) per ply provided by the Hashin's criterion are shown in Figures 3 and 4 for CFRP and FFRP laminates, respectively. In both laminates, the nodal line A and the ply angle 0° are shown to be the most critical. The minimum values in the CFRP and FFRP laminates are -16 % and -51 %. This indicates that the applied loading provides the damage onset for both laminates based on the Hashin criterion. However, the loading is more critical to the FFRP laminate.

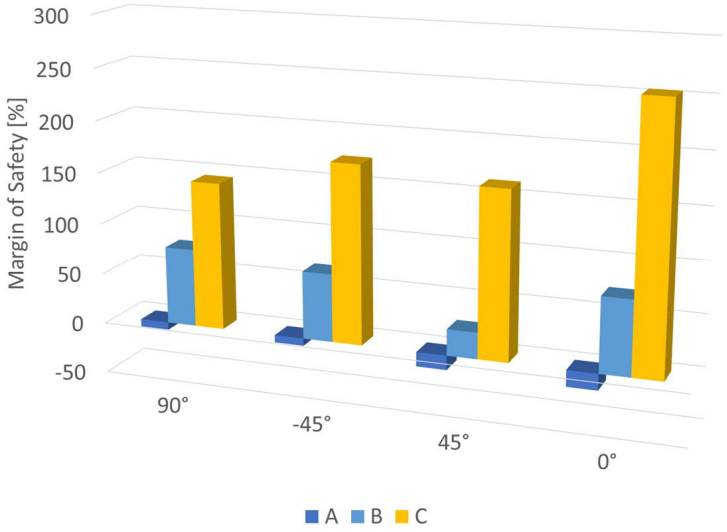

Figure 3. The margin of safety provided by the Hashin criterion's maximum value for the four-ply angles and three nodal lines in the CFRP laminate.

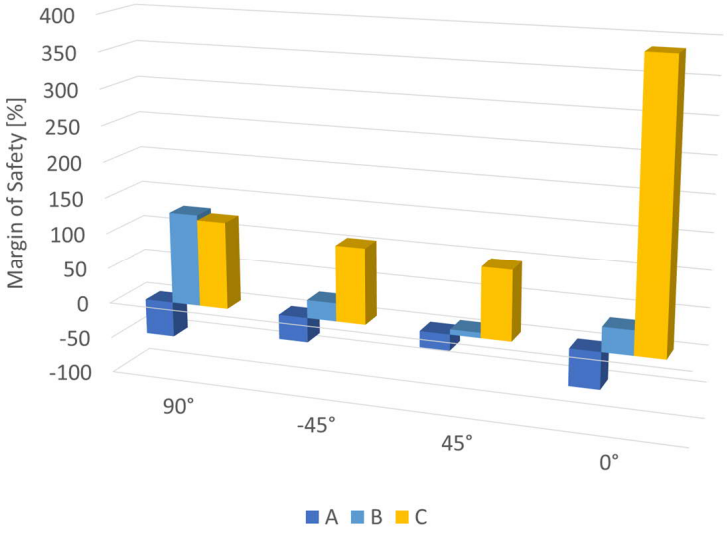

Figure 4. The margin of safety provided by the Hashin criterion's maximum value for the four-ply angles and three nodal lines in the FFRP laminate.

3.3 Puck criterion

Secondly, the Puck stress criterion was used in the analysis. The Puck criterion-related analyses for the CFRP and FFRP laminates are shown in Figures 5 and 6. The Puck criterion has parameters in it, which were modified during the analyses. In the CFRP laminate (Figure 5), the parameters

influence was around 5 % among the results gained. The comparison to the Hashin criterion remarked a difference of 10 % when compared to the highest value (of criterion) provided by the Puck criterion.

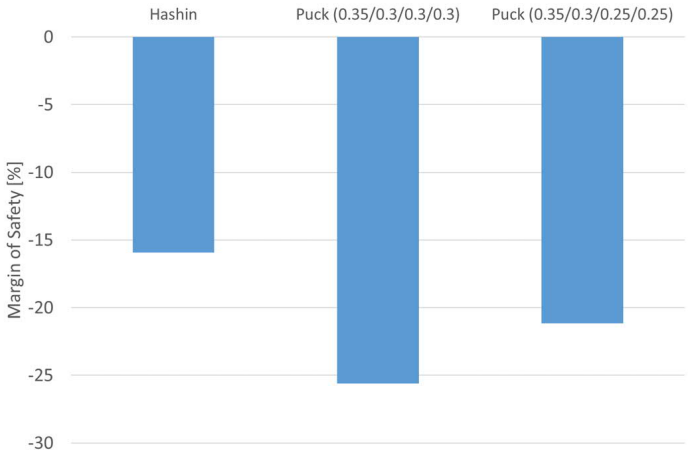

Figure 5. The influence of the Puck criterion's parameters on the MoS and its comparison to the MoS by the Hashin criterion for the CFRP laminate.

The Puck parameters are typically provided for CFRP and glass FRP (i.e., GFRP) laminates. In the FFRP laminate case of this study, both GFRP and CFRP parameters were used. The CFRP parameter values (0.35/0.3/0.3/0.3) provided the values close to the Hashin's criterion. The GFRP parameter values (0.3/0.25/0.2/0.2) provided almost a 10 % difference (at a maximum). The GFRP values lead to more conservative prediction of failure.

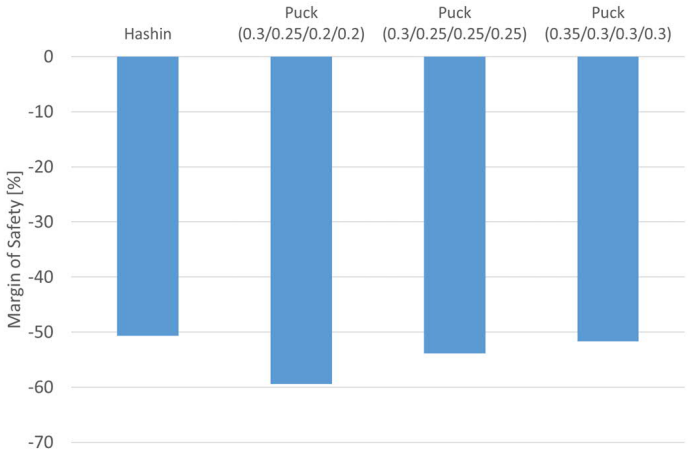

Figure 6. The influence of the Puck criterion's parameters on the MoS and its comparison to the MoS by the Hashin criterion for the FFRP laminate.

3.4 Friction and pressure

Finally, friction and rivet pressure were analysed. These analyses were performed using the Hashin criterion. The results for the CFRP and FFRP joints are shown in Figures 7 and 8. According to the results, friction has an influence on the MoS of the laminate. The pure (emulated tightening) pressure did not provide significant change for the MoS of the laminate. For that reason, only the combination of friction and pressure is provided in the results in Figures 7 and

Error! Reference source not found.. This combination improves the MoS value. Results clearly indicate that the friction distributes the loading over a large area, and the rivet is less loaded.

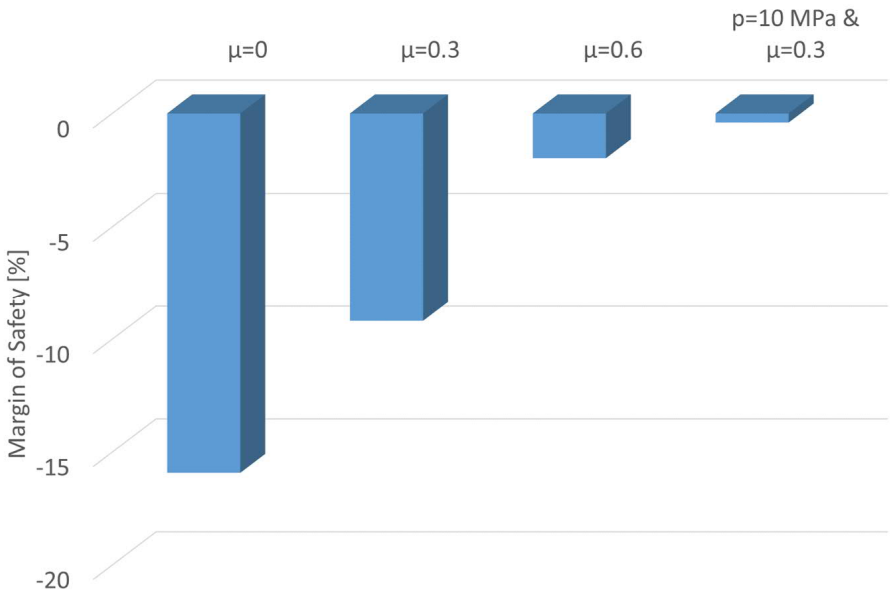

Figure 7. The effect of joint friction and rivet pressure on the MoS of CFRP laminate.

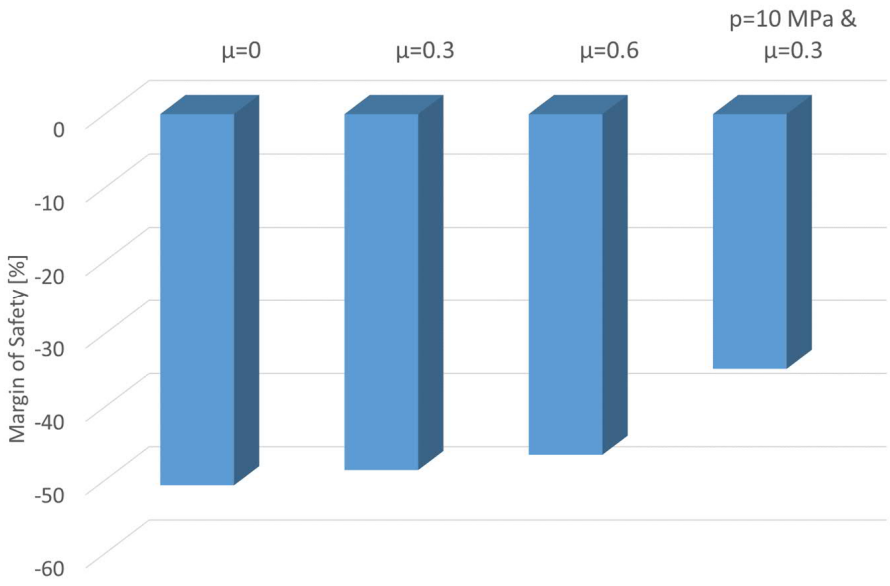

Figure 8. The effect of joint friction and rivet pressure on the MoS of FFRP laminate.

4. Conclusion and discussion

In this work, the damage onset in mechanical joints with composite laminates and fasteners was studied. The damage onset was based on two stress-based criteria, Hashin 3D and Puck. The criterion is using stress components provided by the finite element used. The stress distribution at the edge of the fastener hole is highly concentrated. Based on the preliminary analyses, the damage onset prediction is highly dependent on the applied finite element mesh. The joint modelling requires modelling the fastener-to-laminate and laminate-to-laminate contacts correctly.

The Hashin 3D criterion in the analysis showed that the loading direction in the fastener hole was the most critical parameter. This states that the bearing stress state would predict the damage onset. The most critical ply angle was 0° in both laminates studied. The damage onset was expected in all the plies. The FFRP laminate's 0° and 90° angles were exceeding the damage onset (prediction) of that made for plies 45° and -45°. The damage onset was more even in the CFRP plies compared to FFRP. The analysis using the Puck criterion resulted in higher values and indicated the likeliness of the damage onset. The parameters (constants) in the Puck criterion were studied in the FFRP plies where established values do not exist and should be covered in future studies. The friction facilitates a uniform stress distribution around the fastener and delays the damage initiation (onset) in the composites. This is a useful result for a practical analysis in that the ignorance of the bearing friction would yield more conservative designs of joints.

Acknowledgements

This research is partly based on the funding related to the ecosystem project SmartTram2 (5136/31/2019) for Tampere University funded by Business Finland.

5. References

[1] Orifici AC, Herszberg I, Thomson RS. Review of methodologies for composite material modelling incorporating failure, Compos Struct 2008;86:194-210.

[2] Fiore V, Calabrese L, Scalici T, Valenza A. Evolution of the bearing failure map of pinned flax composite laminates aged in marine environment. Compos Part B Eng 2020;187:107864.

[3] Estrada RG, Santiuste C, Barbero E. Failure maps of biocomposites mechanical joints reinforced with natural fibres. Compos Part C Open Access 2021;5:100159.

[4] Skytta V, Saarela O, Wallin M. Progressive Failure of Composite Laminates; Analysis vs Experiments. Fract Nano Eng Mater Struct - Proc 16th Eur Conf Fract 2006:341–2.

[5] Javanshour F, Prapavesis A, Pärnänen T, Orell O, Lessa Belone MC, Layek RK, et al. Modulating impact resistance of flax epoxy composites with thermoplastic interfacial toughening. Compos Part A Appl Sci Manuf 2021;150:106628.

[6] Prapavesis A, Tojaga V, Östlund S, Willem van Vuure A. Back calculated compressive properties of flax fibers utilizing the Impregnated Fiber Bundle Test (IFBT). Compos Part A Appl Sci Manuf 2020;135:105930.

[7] Hashin Z. Failure criteria for unidirectional fiber-reinforced materials, J Compos Mater, 1980;7:48-464.

[8] Puck A, Schürmann H. Failure analysis if FRP laminates by mans of physically based phenomenological models, Compos Sci Technol, 1998;58:1045-1067.

[9] Rodera Garcia O. Damage onset modelling of curved composite laminates. Master of Science thesis, Tampere University of Technology, 2018.

  doi:10.5075/epfl-298799_978-2-9701614-0-0